Korean Journal of Remote Sensing, Vol.18, No.5, 2002, pp.243~253

Geostrophic Velocities Derived from Satellite Altimetry in the Sea South of Japan

Seung-Bum Kim

Satellite Technology Research Center, Korea Advanced Inst. Science and Tech.

Abstract : Time-mean and absolute geostrophic velocities of the Kuroshio current south of Japan are derived from TOPEX/Poseidon altimeter data using a Gaussian jet model. When compared with simultaneous measurements from a shipboard acoustic Doppler current profiler (ADCP) at two intersection points, the altimetric and ADCP absolute velocities correlate well with the correlation coefficient of 0.55 to 0.74. The accuracy of time-mean velocity ranges from 1 cm s^{-1} to 5 cm s^{-1}. The errors in the absolute and the mean velocities are similar to those reported previously for other currents. The comparable performance suggests the Gaussian jet model is a promising methodology for determining absolute geostrophic velocities, noting that in this region the Kuroshio does not meander sufficiently and thus provides unfavorable environment for the performance of the Gaussian jet model.

Key Words : Geostrophic Velocity, Satellite Altimetry, Kuroshio Current, Gaussian Jet Model.

1. Introduction

The major components of ocean currents are driven by wind and buoyancy. The wind driven component can be divided further into geostrophic and Ekman currents, referring to flow associated with press-balance within the ocean and wind-friction respectively. In the North Pacific, for example, the buoyancy-driven current is near zero and the geostrophic current is the most dominant component of ocean currents: geostrophic and Ekman currents explain 28 Sv (=10^6 m^3 s^{-1}) and 12 Sv of the depth-integrated flow (Bryden *et al.*, 1991), respectively.

The Kuroshio current is one of the main geostrophic current systems in the North Pacific and is important for ocean circulation and climate: e.g., meridional heat flux, upper ocean temperatures and global-scale teleconnections. Thus significant efforts have been paid to measure its absolute velocity and transport (e.g., Hanawa *et al.*, 1996). Numerous methods to measure a current velocity have merits and drawbacks of their own: such as the need of a reference velocity, the geoid or in situ measurements as drawbacks. Among these, the Gaussian jet model for deriving the velocity from satellite altimetry data, proposed by Kelly and Gille (1990, hereafter KG) and improved by Qiu (1995) and Kim and Saunders (2002), is advantageous because it requires none of the drawbacks and is relatively simple. Though the method is limited to regions of strong

Received 15 August 2002; Accepted 25 September 2002.

current meandering, its utility has been widely demonstrated in the measurement of the major current systems in the world ocean: the Gulf Stream (Kelly *et al.*, 1991), the Kuroshio Extension (Qiu, 1995), and the Antarctic Circumpolar Current (Gille, 1994).

Although the performance of the Gaussian jet model has been assessed many times (Joyce *et al.*, 1990; Kelly *et al.*, 1991; Gille, 1994), its accuracy for the Kuroshio current is not available. The Kuroshio to the south of Japan has relatively stable path and in this case the Gaussian jet model may not perform well because it requires strong meandering. In this work, therefore, we aim at deriving the absolute geostrophic of the Kuroshio current using the altimeter records from TOPEX/Poseidon (T/P) satellites and assess its performance by comparing with in-situ measurements by an acoustic Doppler current profiler (ADCP).

2. Data and Method

1) T/P Data Preparation

T/P sea surface height (SSH) data used in this study are one-per-second geophysical data records (GDRs) for cycles 001 to 110. Standard editing procedures and corrections are applied as suggested by AVISO (Archiving, Validation and Interpretation of Satellites Oceanographic data) team of CNES (Centre National d'Etudes Spatiales), France. These are as follows: we use NASA altitude for the orbit; the Ku band for the range; the radiometer wet tropospheric correction for the wet correction; the dry meteorological tropospheric correction for the dry correction; the TOPEX dual-frequency once-per-frame correction for the ionospheric delay; and the Cartwright and Ray model for ocean tide correction (Cartwright and Ray, 1990). Further we apply the waveform center of gravity correction, the solid earth tide correction, the pole tide correction; and the inverse barometer correction. The consequent data are comparable with the GDR version C. The raw GDR SSH records are collocated onto ground tracks of T/P cycle 018. Then residual SSHs from the mean sea surface elevation are computed using a collinear method. To remove the instrument noise, the raw altimeter data are smoothed using a Gaussian filter with a the full width at half-power point (L_{HM}) of 63 km, which is found optimal (Kim and Saunders, 2002).

2) ADCP Records

To assess the performance of the Gaussian jet model, we compare the velocity derived from the model with in situ velocity from ADCP observations at three intersection points (Fig. 1). The ADCP measurements have been made every three days continuously from February 1991 except for a two-month data gap in 1995. Raw data measurements are taken every 16 m from the surface down to a nominal 400 m depth with a sample averaging interval of five minutes (see Hanawa *et al.*, 1996, for the full details of the raw data). Misalignment error between the ship heading and the ADCP coordinate system is eliminated by assuming the currents do not change between two consecutive cruises

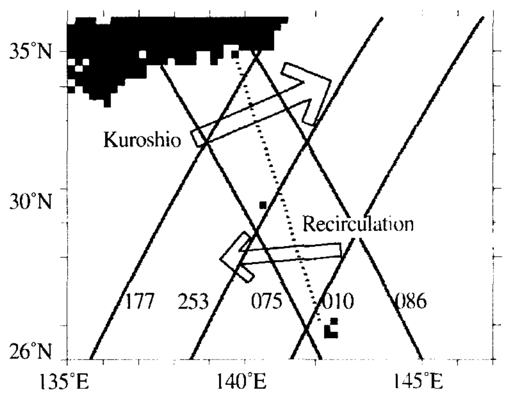

Fig. 1. Ship track for ADCP measurements (sparse dots) and T/P ground tracks (dense dots). The three digit numbers inside the panel indicate the T/P ground track numbers.

that are separated by a week. To eliminate the influence of the Ekman current the ADCP measurements are taken at 47 m depth are used. Removal of tidal components is achieved by taking a temporal average with a Gaussian filter having an e-folding scale of 15 days and the final ADCP products are available every 15-day interval. The M2, N2, K2, O1 and Q1 tides are removed further by Gaussian smoothing and harmonic analysis.

3) Implementation of Gaussian Jet Model

In the Gaussian jet model, the time-mean current is reconstructed iteratively from the temporal anomaly using a Gaussian profile for the cross-stream absolute geostrophic velocity at the surface. Having reconstructed the mean current, by adding the temporal anomaly to it, the absolute geostrophic current may be obtained. The Gaussian model is given as (KG)

$$u_s(y,t) = a_1(t)\exp\left[\frac{-(y-a_2(t))^2}{2a_3(t)^2}\right], \qquad (1)$$

where $a_1(t)$ is the peak velocity of the jet, $a_2(t)$ its axis position, and $a_3(t)$ its width. us denotes an absolute velocity synthesized using a_1, a_2 and a_3. We model the recirculations in the northern and southern sides of the jet following Qiu (1995): linear function of the distance from the jet center, constrained by climatology at 25°N and 40°N. The fundamental idea behind this method is that the velocity anomaly is representative of the absolute velocity in terms of a_2 and a_3 if the jet meanders a distance of order its typical width (Fig. 2). For more details of the implementation and improvement to the KG-Qiu's implementation, one may refer to Kim and Saunders (2002).

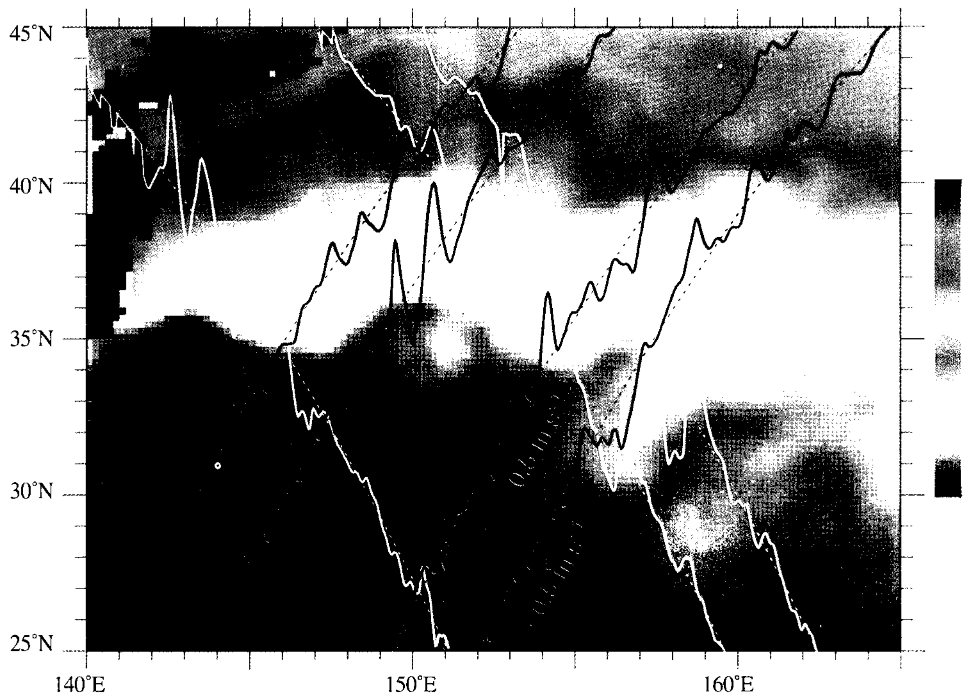

Fig. 2. Velocity anomalies from T/P records superimposed on a simultaneous sea surface temperature (SST) image from the ERS-1 satellite. The T/P data come from cycle 035 (Sept. 1993). SST scale on the left indicates 30°C for dark red to 0°C for purple.

3. Comparison of Absolute Geostrophic Velocities

In comparing the time series of the altimetric and ADCP velocities, for synchronization between the two velocities, we average the altimetric velocities over three T/P 10-day repeat cycles with uniform weights and interpolate three bi-monthly ADCP velocities onto mid-month using weighting values of 0.25, 0.5 and 0.25. For collocation we average five T/P velocities near the intersection point spatially, because the T/P velocities are given every 5.7 km along-track and the L_{HM} of the spatial smoothing filter for the ADCP data is 31 km.

At the intersection point on ground track 177, the two velocities correlate reasonably well at the correlation coefficient of 0.55 (Fig. 3a). The velocities around

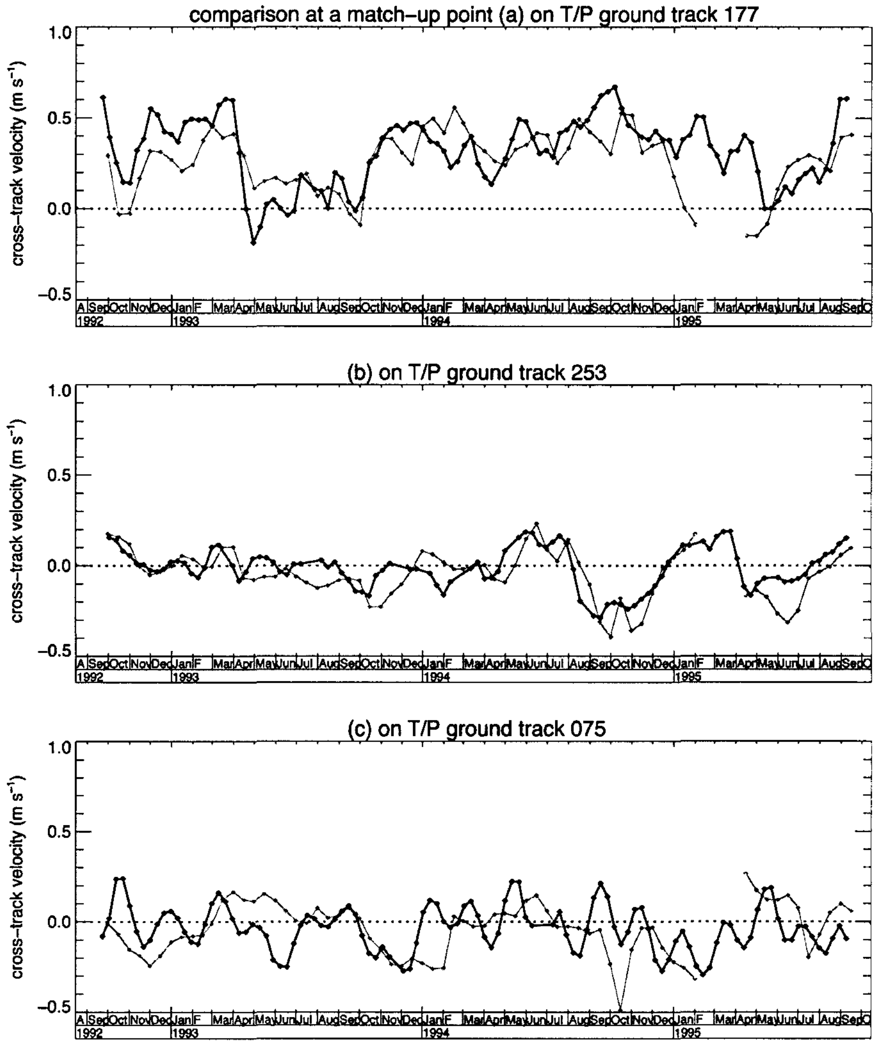

Fig. 3. Comparison of cross-track absolute geostrophic velocities at the intersection points between the Gaussian jet method output (black) and the ADCP measurements (gray). The gap around March 1995 indicates missing data. The velocity is positive if eastward.

summer 1993 are smaller than those in other periods. Around summer of 1993 the Kuroshio takes an offshore path: its axis on the ADCP ship track moves to about 33°N. Thus the Kuroshio velocity at the 34°10′N intersection point tends to be smaller (Fig. 4a) than normal (Fig. 4b). However, in September 1993, even if the current is on the nearshore path (Fig. 4c), the velocities are small. This is because the current direction is almost parallel to the T/P ground track (Fig. 4c). Some of the large differences between the two velocities are observed during the offshore path: October 1992 and May 1993. In this case the path of the Kuroshio near the intersection point is quite variable (compare Fig. 4a and Fig. 4d), and the velocities would be susceptible to difference in sampling time between the altimetric and ADCP observations.

On ground track 253 the two time series agree very well with a correlation coefficient of 0.74 (Fig. 3b). The westward (negative) velocities indicate the recirculation gyre, the typical position of which is 29°N along the ADCP line (Ebuchi and Hanawa, 2000, Fig. 1). Also meso-scale eddies are captured in the time series: the large negative velocity in fall 1994 and the positive blob in October 1992 represent cyclonic and anticyclonic eddies respectively (Ebuchi and Hanawa, 2000).

The comparison on ground track 075 is poor (Fig.

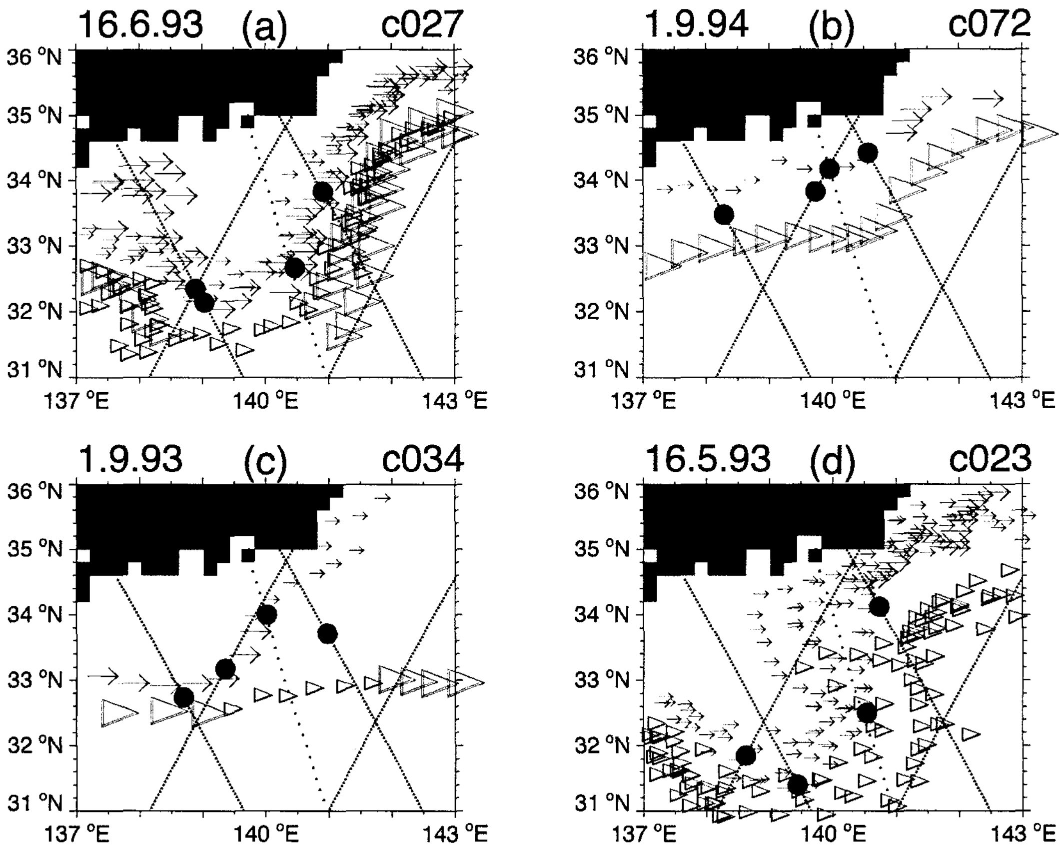

Fig. 4. Positions for the Kuroshio path monitored by the Gaussian jet model and the ADCP records (solid circles) and AVHRR sea surface temperature frontal positions (arrows and triangles for the north and south walls respectively). The title indicates the dates and the cycle number of T/P altimeter.

Table 1. Errors in SSH Rise across Jet or Cross-track Velocity Determined using Gaussian Jet Method. Measures of the differences are given in parenthesis, next to the corresponding percentages (relative to the root-mean-square of the signal). GS, ACC, and KU stand for the Gulf Stream, the Antarctic Circumpolar Current, and the Kuroshio respectively.

Authors	Area	Difference (altimetric - ADCP)		Source of 'truth' data
		Mean	r.m.s.	
Joyce *et al.* (1990)	GS	n/a	48 % (23 cm s^{-1})	ADCP
Kelly *et al.* (1991)	GS	15%(11 cm)	N/a	ADCP
Gille (1994)	ACC	7%(3.0 cm)	N/a	Simulation
This study				
Ground Track 177	KU	15% (5.4 cm s^{-1})	48 % (17.6 cm s^{-1})	ADCP
Ground Track 253	KU	23% (2.9 cm s^{-1})	73 % (9.1 cm s^{-1})	ADCP
Ground Track 075	KU	7% (1.0 cm s^{-1})	133 % (18.8 cm s^{-1})	ADCP

3c). This results from the combined effect of weak signal and the comparatively large random error. The location of the intersection point on ground track 075 is about 500 km south of the offshore location of the Kuroshio. Consequently the signal is weak. On the other hand, the difference in standard deviation is large (18.8 cm s^{-1}, Table 1). These indicate that most of the anomalous fluctuations are random.

Table 1 shows that the r.m.s. difference found on ground track 177 agrees with the estimate found by Joyce *et al.* (1990). To understand the size of the r.m.s. difference, let us analyze its sources. Since the mean difference is small compared with the r.m.s. difference, we may analyze the difference in standard deviation instead. The main sources of the difference include:

(i) the precision of the T/P altimeter measurement. The T/P point measurement precision is 4.1 cm and 5.1 cm for TOPEX and Poseidon, respectively (Fu *et al.*, 1994). For convenience 5.0 cm is used in the following calculations. The precision in the corresponding velocity anomaly is 1.4 m s^{-1}, based on geostrophy and the T/P spatial sampling interval of 5.7 km. After the Gaussian pre-smoothing with the 63-km L_{HM}, the spatial averaging of five T/P records and the monthly averaging, the precision in T/P velocity anomaly is reduced to 11 cm s^{-1}.

(ii) the precision of the Gaussian jet model, that is, the random error in the mean velocity estimated by the model. An estimate of this error would require either a simulation of noise as in Gille (1994) or a comparison of the KG mean velocities with in situ mean velocities on a statistically sufficient number of locations where the mean velocities are validated. Since neither of these has been performed in the current study, Gille's estimate of 12% (7.7 cm) will be used. The precision of the Gaussian jet model implemented in this study is expected to be better than 12 % for the following two reasons. Firstly, the magnitude of the perturbation noise used in Gille's Monte-Carlo simulation would be smaller for T/P data because the T/P measurements are of higher precision than the Geosat records used by Gille. Secondly, the KG method would perform better for the Kuroshio than for the Antarctic Circumpolar Current (ACC) studied by Gille because the ACC has a weaker strength but more complicated velocity structure.

(iii) the precision of the ADCP measurements. This is estimated to be 4.5 cm s^{-1} (Hanawa *et al.*, 1996), reflecting that 1° misalignment between the ship heading and the ADCP reference gives 18 cm s^{-1} and the standard deviation of the angle correction scatters by 0.25°.

Combining the contributions from the three sources above gives 12 cm s^{-1} for the difference in standard deviation between the absolute monthly KG velocity and the ADCP velocity. This value is comparable with the observed values for the difference in standard deviation for the three intersection points: 8.6 cm s^{-1} to 18.8 cm s^{-1} that can be computed from Table 1.

4. Comparison of Time-mean Geostrophic Velocity

The intersection point on T/P ground track 177 is a favorable location for assessing the performance of the Gaussian jet model for the main jet because the point is located within the jet (the main jet is shown in Fig. 1 and its cross-stream profile is defined in Eq. (1)). The mean difference at the intersection points on the track 177 is 5.4 cm s^{-1}, 15% of the signal (Table 1). The 15% difference is attributed to the combination of intrinsic errors in the Gaussian jet model, noise in the altimeter records and the consequent deterioration of the model's performance, and insufficient meandering of the Kuroshio to the south of Japan. The insufficient meandering is manifested by the fact that the path of the Kuroshio along T/P ground track 177 has two preferred locations as shown in Fig. 4. This quasi-stability will result in a weak velocity anomaly and, consequently, poor performance of the Gaussian jet model. Gille (1994) and Kim and Saunders (2002) quantify the sizes of these three error terms by simulation and they are estimated to 0.6%, 5.0% and 5.5% of the signal respectively. The quadrature addition of these three sources produces an error budget of 7.5%.

How does our assessment of the Gaussian jet model for the Kuroshio compare with those made for other current systems? In terms of the mean difference this study on ground track 177 and Kelly *et al.* (1991) give a larger error budget than in Gille (1994, Table 1). The reason is that Gille's Monte-Carlo simulation accounts for intrinsic errors in the Gaussian jet model and noise in the altimeter records. By comparison, the mean difference values in this study and in Kelly *et al.* additionally include potential errors in the reference ADCP data. Furthermore, our study accounts for the errors due to quasi-stable meandering of the jet. Thus it would be reasonable to maintain that the accuracy of the Gaussian jet method on the Kuroshio from our study is comparable with that on the GS and ACC by Kelly *et al.* (1991) and Gille (1994). The mean difference on ground track 177 from this study agrees well with the validation result of Kelly *et al.* (1991). This suggests the Gaussian jet model is robust even to the insufficient meandering of the Kuroshio (the GS validation was conducted in the open ocean where it meanders sufficiently).

At the intersection points on T/P ground tracks 075 and 253 we may assess the performance of the recirculation model since below ~31°N the flow pattern is dominated by the westward recirculation (Fig. 1). The mean difference ranges from 1.0 cm s^{-1} to 2.9 cm s^{-1} (Table 1) or 7% to 23% of the signal. Such level of difference is very encouraging noting that the recirculation model is just a simple linear one.

5. Summary and Discussions

We have derived the absolute geopstrophic velocity from T/P altimeter records and assessed its accuracy for the Kuroshio current and its recirculation to the south of Japan. At two intersection points between ADCP ship track and T/P ground track, the altimetric and ADCP velocities agree well with correlation coefficients of 0.56 and 0.71 at > 99 % significance. The mean velocities between the T/P and ADCP derivations at the intersection points differ by 1 cm s^{-1} to 5 cm s^{-1}. These differences are comparable with those for the Gulf Stream. Noting that the insufficient meandering of the

Kuroshio would provide unfavorable environment for the performance of the Gaussian jet model, the similar level of performance for the Kuroshio and the Gulf Stream suggests the robustness of the Gaussian jet method. We further found that the simple model for the recirculation is effective.

The difference in standard deviation between the altimetric and ADCP velocities reached 18.8 cm s^{-1}, out of which we identified the causes of 12 cm s^{-1} in Section 3. Could the remainder be due to any errors in the ADCP data? We assume that if the ADCP error is zero, the Kuroshio mass transport across the ADCP ship track should remain constant in time. The basis of this assumption is that the dominant periodicity of the Kuroshio mass transport is annual and thus intra-annual variation should be small. On this ground, the time interval of such mass conservation constraint is set to be smaller than a year and the same as the interval of the ADCP data - 15 days. We note that the mass transport value is not available directly from the ADCP data. Thus we infer the mass transport using the SSH rise across the ADCP ship track, based on the geostrophic relationship:

$$\begin{aligned} \text{surface transport} &= -g/f \times \int u dl \\ &= -g/f \times \text{SSH rise across ADCP track,} \end{aligned} \tag{2}$$

where the surface transport is the mass transport within the top 1 m of the ocean, u is the velocity across the ADCP track, g the gravitational constant and f the Coriolis parameter. And further, to the south of Japan,

$$\text{mass transport (depth-integrated)} \approx \text{surface transport.} \tag{3}$$

This approximation is supported by the observations of Imawaki *et al.* (2001). Based on the above assumption and Eqs. (2) and (3), we have examined

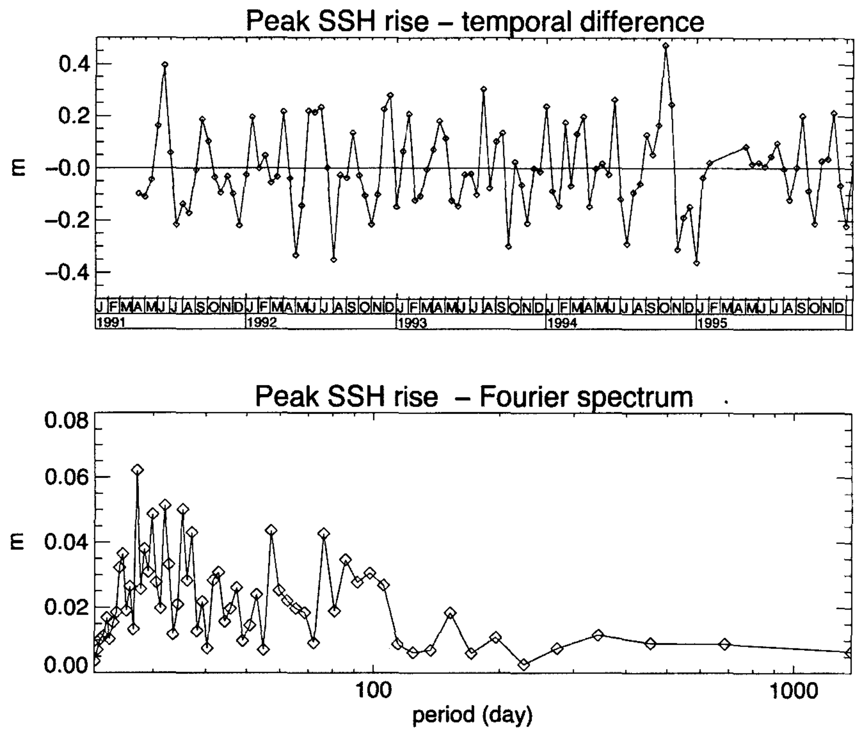

Fig. 5. Temporal variations in the peak SSH rise across the ADCP ship track: (a) time series and (b) amplitude of Fourier spectrum computed using the time series from March 1991 to January 1995.

whether the mass transport is constant in time, using the SSH rise parameter. We find that the SSH rise is not constant in time (Fig. 5a) and it shows periodic signals. The frequency spectrum in Fig. 5b shows the peaks at the periods from 60 to 100 days and the peak at 360 days. The 360-day peak appears attenuated because of the differencing operation: $\delta(\sin\omega t) = \omega\cos\omega t$ and ω becomes smaller as the period increases. The short-period peaks would be noise, e.g., the 15-day peak as in Fig. 4 of Ebuchi and Hanawa (2000).

Possible causes of the periodicity in Fig. 5a include steric effect, tides, variations in Kuroshio transport, variations in recirculation, Rossby waves, and meso-scale eddies. Steric effect is not expected to be the reason because it has an annual cycle (360-day period), and it does not affect the SSH rise because solar heating may be regarded uniform over a small scale like the study area. There are no significant tides with periods of 60 ~ 100 days.

To examine the impact of wind forcing on the Kuroshio variations we computed the frequency spectrum of wind forcing or equivalently the Sverdrup transport. The strong signal at 60-day period (Fig. 6) would be the cause of the 60-day signal observed in the ADCP SSH variations in Fig. 5a. Identification of the causes of this periodicity remains as a future work. The 360-day signal is found strong in the Sverdrup transport, which would be the cause of the same periodicity in the ADCP SSH variations. The Sverdrup transport is greater at 270 days than at 360 days, which is not understood at present.

Westward recirculation is driven according to anticyclonic genesis (Worthington, 1976) or the local instability (Qiu and Miao, 2000). These causes have time scales of a year and ~4 years respectively, and thus the recirculation is not likely to explain the 60 ~ 100 day periodicity in our observations.

Rossby waves are generated by wind bursts and topographic effect. We expect that wind bursts are more irregular and concentrated in winter than are periodic. Izu Ridge, which runs parallel to the ADCP ship track to the east of the track, does indeed generate westward propagation of Rossby waves at the speed of 1st barotropic mode (Isobe and Imawaki, 2002). But in this case, wind forcing is a prerequisite and, as shown in Fig. 6, the periodicity of the wind can explain only the 60-day periodicity.

Finally Ebuchi and Hanawa (2000, 2001) analyze the same ADCP data as used in this study and altimeter data. They found that meso-scale eddies have frequencies of 50 ~ 80 days over the time span of this study. The eddies are generated in the south of the

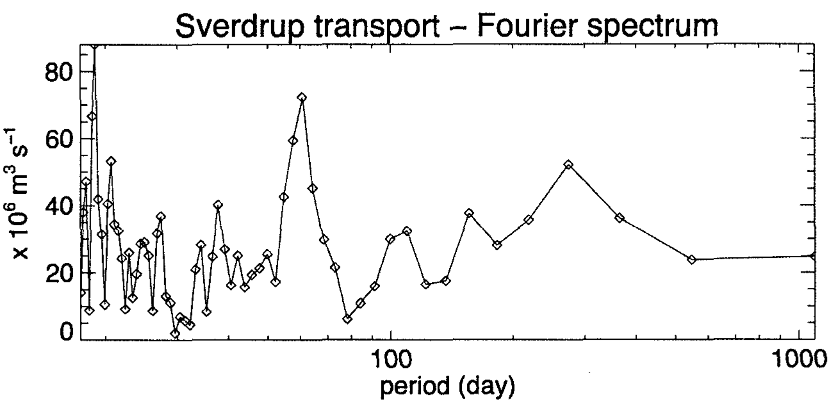

Fig. 6. Fourier spectrum of Sverdrup transport at 130°E, 30°N - the location of the largest Sverdrup transport in the North Pacific.

Kuroshio Extension by pinching off from the jet. They found that the eddies perpendicularly cross the ADCP section because of topographic steering and, in doing so, perturb the SSH rise across the ADCP track. The perturbation to the SSH has the size of about 10 cm, similar to the size of the variations in Fig. 5a. Eddies also affect the Kuroshio variations directly by impinging on it (Ebuchi and Hanawa, 2002, in the South of Japan; Gilson and Roemmich, 2002, south of Taiwan). The 7-year hydrographic observations of eddies by Gilson and Roemmich (2002) report 100-day periodicity, which matches with our observation in Fig. 5b. But further analysis is required to fully address how the eddy impinging on the Kuroshio influences our observations south of Japan.

In the future, we will analyze further the periodic variations in SSH rise observed in Fig. 6. If we fully identify causes of the periodicity, the next step is to correct the 15-day interval ADCP data for the causes. Such correction may result in better comparison in the velocities between the altimetric and ADCP solutions.

Acknowledgements

This research was supported by the following research projects at SATREC, funded by the Ministry of Science and Technology and the Ministry of Information and Telecommunication, S. Korea: 'Development and utilization of a ground terminal for low-earth orbit satellites' and 'Construction of satellite data receiving structure'. Discussions and comments by N. Ebuchi and K. Hanawa were very helpful. We appreciate data provision from the following: the AVISO team of CNES for T/P data; K. Hanawa of the Tohoku Univ. for the ADCP data.

References

Bryden, H.L., D.H. Roemmich and J.A. Church, 1991. Ocean heat transport across 24°N in the Pacific, *Deep-Sea Research*, 38: 297-324.

Cartwright, D.E. and R.D. Ray, 1990. Ocean tides from Geosat altimetry, *Journal of Geophysical Research*, 90: 3069-3090.

Ebuchi, N. and K. Hanawa, 2000. Mesoscale eddies observed by TOLEX-ADCP and TOPEX/POSEIDON altimeter in the Kuroshio recirculation region South of Japan, *Journal of Oceanography*, 56: 43-57.

__________________, 2001. Trajectory of mesoscale eddies in the Kuroshio recirculation region, *Journal of Oceanography*, 57: 471-480.

__________________, 2002. Influence of mesoscale eddies on variations of the Kuroshio path south of Japan, *Journal of Oceanography*, in press.

Fu, L.-L. and coauthors, 1994. TOPEX/POSEIDON mission overview, *Journal of Geophysical Research*, 99: 24 369-24 383.

Gille, S.T., 1994. Mean sea-surface height of the Antarctic Circumpolar Current from Geosat data - method and application, *Journal of Geophysical Research*, 99: 18 255-18 273.

Gilson, J. and D. Roemmich, 2002. Mean and temporal variability in Kuroshio geostrophic transport south of Taiwan (1993-2001), *Journal of Oceanography*, 58: 183-195.

Hanawa, K., Y. Yoshikawa and T. Taneda, 1996. TOLEX-ADCP monitoring, *Geophysical Research Letters*, 23: 2429-2432.

Isobe, A. and S. Imawaki, 2002. Annual variation of the Kuroshio transport in a two-layer numerical model with a ridge, *Journal of Physical Oceanography*, 32: 994-1009.

Imawaki, S. and ASUKA group, 2001. Satellite altimeter monitoring the Kuroshio transport south of Japan, *Geophysical Research Letters*, 28: 17-20.

Joyce, T.M., K.A. Kelly, D.M. Schubert and M.J. Caruso, 1990. Shipboard and altimetric studies of rapid Gulf Stream variability between Cape Cod and Bermuda, *Deep-Sea Research*, 37: 897-910.

Kelly, K.A. and S.T. Gille, 1990. Gulf Stream surface transport and statistics at 69°W from the Geosat altimeter, *Journal of Geophysical Research*, 95: 3149-3161.

_____, T.M. Joyce, D.M. Schubert and M.J. Caruso, 1991. The mean sea surface height and geoid along the Geosat subtrack from Burmuda to Cape Cod, *Journal of Geophysical Research*, 96: 12 699-12 709.

Kim, S.B. and M.A. Saunders, 2002. An improved Gaussian jet model for deriving absolute geostrophic velocity from satellite altimetry, *Journal of Atmospheric and Oceanic Technology*, 19: 2020-2029.

Qiu, B., 1995. Variabilities and energetics of the Kuroshio Extension and its recirculation gyre from the first two-year TOPEX data, *Journal of Physical Oceanography*, 25: 1827-1842.

_____ and W.F. Miao, 2000. Kuroshio path variations south of Japan: Bimodality as a self-sustained internal oscillation, *Journal of Physical Oceanography*, 30: 2124-2137.

Worthington, L.V., 1976. *On the North Atlantic Circulation.*, Johns Hopkins University Press, Baltimore, p.110.